

FUZZY LOGIC BASED ADAPTATION MECHANISM FOR ADAPTIVE LUENBERGER OBSERVER SENSORLESS DIRECT TORQUE CONTROL OF INDUCTION MOTOR

A. BENNASSAR*, A. ABBOU, M. AKHERRAZ, M. BARARA

Department of Electrical Engineering, Mohammed V University Agdal,
Mohammadia School's of Engineers, Street Ibn Sina B.P 765 Agdal Rabat, Morocco

*Corresponding Author: ab.bennassar@gmail.com

Abstract

Many industrial applications require high performance speed sensorless operation and demand new control methods in order to obtain fast dynamic response and insensitive to external disturbances. The current research aims to present the performance of the sensorless direct torque control (DTC) of an induction motor (IM) using adaptive Luenberger observer (ALO) with fuzzy logic controller (FLC) for adaptation mechanism. The rotor speed is regulated by proportional integral (PI) anti-windup controller. The proposed strategy is directed to reduce the ripple on the torque and the flux. Numerical simulation results show the good performance and effectiveness of the proposed sensorless control for different references of the speed even both low and high speeds.

Keywords: Sensorless direct torque control, Induction motor, adaptive Luenberger observer, Fuzzy logic controller, PI anti-windup.

1. Introduction

The induction motor is one of the most widely used machines in various industrial applications due to its high reliability, relatively low cost, and modest maintenance requirements [1].

The nonlinear structure of the induction motor requires decoupled torque and flux control. This control is provided through field oriented control (FOC) [2, 3]. However, the FOC scheme requires current controllers and coordinates transformations. This problem is avoided by direct torque control technique (DTC) [4]. The DTC technique provides a very fast torque and flux control without the inner current regulation loop [5, 6]. The disadvantages of conventional

Nomenclatures

C_e	Electromagnetic torque, N.m
$i_{s\alpha,\beta}$	Stator current in the stationary α, β axis, A
L_s, L_r, L_m	Stator, rotor and mutual inductances, H
P	Number of pole pairs
R_s, R_r	Stator and rotor resistances, Ω
T_e	Period of sampling, s
L	Observer gain matrix
T_r	Rotor time constant, H/ Ω
$u_{s\alpha,\beta}$	Stator voltage in the stationary α, β axis, V

Greek Symbols

ϕ_r	Rotor flux, Wb
ω_r	Rotor speed, rad/s
$\phi_{r\alpha,\beta}$	Rotor flux in the stationary α, β axis, Wb
ϕ_s	Stator flux, Wb
σ	Leakage coefficient

Abbreviations

ALO	Adaptive Luenberger Observer
DTC	Direct Torque Control
FLC	Fuzzy Logic Control
FOC	Field Oriented Control
IM	Induction Motor

DTC are high torque ripple and slow transient response to the step changes in torque during start-up [7, 8]. For that reason, the application of PI anti-windup controller for speed regulation consists in correcting the integral action.

On the other hand, the sensorless speed control of induction motor has received over the last few years a great interest. Thus it is necessary to eliminate the speed sensor to reduce hardware and increase mechanical robustness without deteriorating the dynamic performance of the drive control system. The adaptive Luenberger observer (ALO) is one of the most techniques used for sensorless induction motor control. It is able to provide both rotor speed and flux without problems of closed-loop integration. In this paper, the fuzzy logic controller (FLC) is used in adaption mechanism for the adaptive Luenberger observer. The main advantages of the FLC that it does not require accurate mathematical model of the induction machine. Fuzzy logic is based on the linguistic rules by means of IF-THEN rules with the human language.

The content of this paper is organized as follow: the induction motor model is described in section two, section three reviews the direct torque control strategy, in section four, the PI ant-windup speed regulator is designed, section five and six develop the adaptive Luenberger observer and fuzzy logic technique respectively, the section seven is devoted to numerical simulation results. Finally, a conclusion ends the paper.

2. Induction Motor Model

A dynamic model of the induction motor in stationary reference frame can be expressed in the form of the state equation as shown below:

$$\begin{cases} \dot{x} = Ax + Bu \\ y = Cx \end{cases} \quad (1)$$

where

$$x = [i_{s\alpha} \quad i_{s\beta} \quad \phi_{r\alpha} \quad \phi_{r\beta}]^t; u = [u_{s\alpha} \quad u_{s\beta}]^t; y = [i_{s\alpha} \quad i_{s\beta}]^t$$

where x , u and y are the state vector, the input vector and the output vector respectively.

$$A = \begin{bmatrix} -\gamma & 0 & \frac{K}{T_r} & K\omega_r \\ 0 & -\gamma & -K\omega_r & \frac{K}{T_r} \\ \frac{L_m}{T_r} & 0 & -\frac{1}{T_r} & -\omega_r \\ 0 & \frac{L_m}{T_r} & \omega_r & -\frac{1}{T_r} \end{bmatrix}; B = \begin{bmatrix} \frac{1}{\sigma L_s} & 0 \\ 0 & \frac{1}{\sigma L_s} \\ 0 & 0 \\ 0 & 0 \end{bmatrix}; C = \begin{bmatrix} 1 & 0 & 0 & 0 \\ 0 & 1 & 0 & 0 \end{bmatrix}$$

with

$$\gamma = \frac{R_s}{\sigma L_s} + \frac{1-\sigma}{\sigma T_r}; K = \frac{L_m}{\sigma L_s L_r}; \sigma = 1 - \frac{L_m^2}{L_s L_r}; T_r = \frac{L_r}{R_r}$$

3. Direct Torque Control Strategy

In a direct torque control technique of induction motor, it is possible to control directly the stator flux linkage and the electromagnetic torque by selecting the appropriate voltage vectors of the inverter. The selection is made to keep the flux and the torque errors within limits of the hysteresis bands. The application of DTC allows very fast torque response without passing by current regulators, PWM pulse generators and coordinate transformations.

3.1. Behaviour of the stator flux

In the stator reference frame, the stator flux can be estimated by the following equation:

$$\bar{\phi}_s = \bar{\phi}_{s0} + \int_0^t (\bar{V}_s - R_s \bar{I}_s) dt \quad (2)$$

The voltage drop due to the resistance of the stator can be neglected (for high speed). The voltage vector applied to the induction machine remains also constant during one period of sampling T_e . Thus, we can write:

$$\bar{\phi}_s = \bar{\phi}_{s0} + \int_0^t \bar{V}_s dt \quad (3)$$

For one period of sampling, the voltage vector applied to the induction machine remains constant, we can write:

$$\bar{\phi}_s(k+1) = \bar{\phi}_s(k) + \bar{V}_s T_e \quad (4)$$

3.2. Behaviour of the torque

The electromagnetic torque is proportional to the vector product of the stator flux and rotor flux:

$$C_e = \frac{pL_m}{\sigma L_s L_r} (\bar{\phi}_s \times \bar{\phi}_r) |\bar{\phi}_s| |\bar{\phi}_r| \sin(\theta_{sr}) \quad (5)$$

where θ_{sr} is the angle between the stator and rotor flux.

3.3. Description of the structure control

Figure 1 shows the selection of the stator voltage V_s which depends on the desired variation of the module of stator flux.

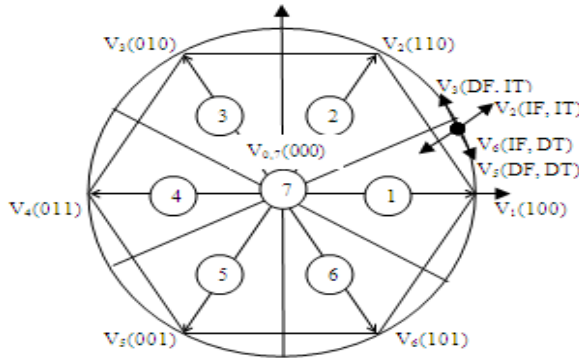


Fig. 1. Selection of voltage vectors.

The electromagnetic torque is controlled by three levels hysteresis comparator illustrated in Fig. 2.

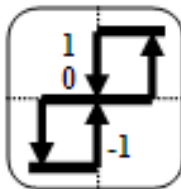


Fig. 2. Three levels hysteresis comparator.

The flux will be compared with the flux reference using two levels hysteresis comparator as shown in Fig. 3. The switching table proposed by Takahashi [3], as given by Table 1. Figure 4 illustrates the global sensorless scheme control used.

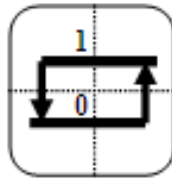


Fig. 3. Two levels hysteresis comparator.

Table 1. Switching table.

$\Delta\phi_s$	ΔC_e	S_1	S_2	S_3	S_4	S_5	S_6
1	1	V_2	V_3	V_4	V_5	V_6	V_1
	0	V_7	V_0	V_7	V_0	V_7	V_0
	-1	V_6	V_1	V_2	V_3	V_4	V_5
0	1	V_3	V_4	V_5	V_5	V_1	V_2
	0	V_0	V_7	V_0	V_7	V_0	V_7
	-1	V_5	V_6	V_1	V_2	V_3	V_4

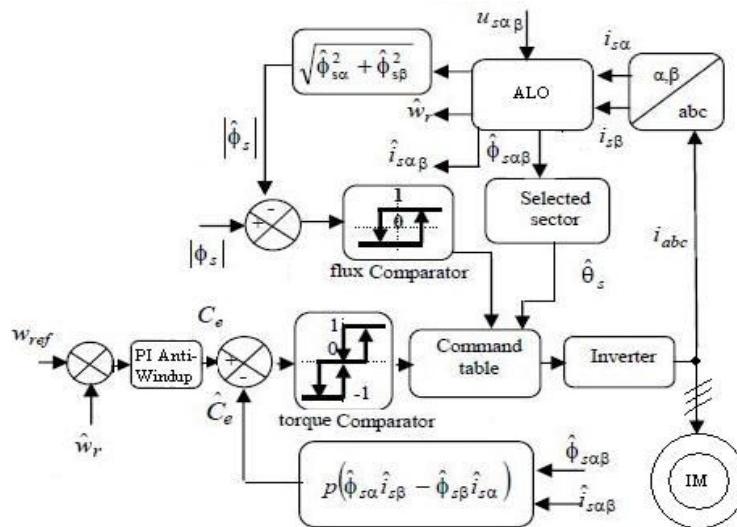


Fig. 4. Block diagram of sensorless control proposed.

4. PI Anti-Windup Regulator

The anti-windup PI regulator is used to correct the integral action according to the diagram of Fig. 5. The correction of the integral action is based on the difference between the values of δ_i upstream and downstream from the limiting device, balanced by the coefficient $1/k_{\rho}$ [9, 10]:

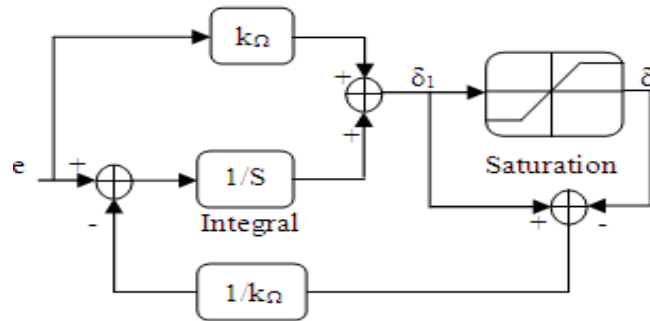


Fig. 5. Structure of the anti-windup PI regulator.

5. Adaptive Luenberger observer

The Adaptive flux observer is a deterministic type of observer based on a deterministic model of the system [11]. In this work, the ALO state observer is used to estimate the flux components and rotor speed of induction motor by including an adaptive mechanism based on the Lyapunov theory. In general, the equations of the ALO can be expressed as follow:

$$\begin{cases} \dot{\hat{x}} = A\hat{x} + Bu + L(y - \hat{y}) \\ \hat{y} = C\hat{x} \end{cases} \quad (6)$$

The symbol $\hat{\cdot}$ denotes estimated value and L is the observer gain matrix. The mechanism of adaptation speed is deduced by Lyapunov theory. The estimation error of the stator current and rotor flux, which is the difference between the observer and the model of the motor, is given by [12]:

$$\dot{e} = (A - LC)e + \Delta A\hat{x} \quad (7)$$

Where

$$e = x - \hat{x} \quad (8)$$

$$\Delta A = A - \hat{A} = \begin{bmatrix} 0 & 0 & 0 & K\Delta\omega_r \\ 0 & 0 & -K\Delta\omega_r & 0 \\ 0 & 0 & 0 & -\Delta\omega_r \\ 0 & 0 & \Delta\omega_r & 0 \end{bmatrix} \quad (9)$$

$$\Delta\omega_r = \omega_r - \hat{\omega}_r \quad (10)$$

We consider the following Lyapunov function:

$$V = e^T e + \frac{(\Delta\omega_r)^2}{\lambda} \quad (11)$$

where λ is a positive coefficient. Its derivative is given as follow:

$$\dot{V} = e^T \{ (A - LC)^T + (A - LC) \} e - 2K\Delta\omega_r (e_{is\alpha} \hat{\phi}_{r\beta} - e_{is\beta} \hat{\phi}_{r\alpha}) + \frac{2}{\lambda} \Delta\omega_r \hat{\omega}_r \quad (12)$$

With $\hat{\omega}_r$ is the estimated rotor speed. The adaptation law for the estimation of the rotor speed can be deduced by the equality between the second and third terms of

Eq. (12):

$$\hat{\omega}_r = \int \lambda K (e_{is\alpha} \hat{\phi}_{r\beta} - e_{is\beta} \hat{\phi}_{r\alpha}) dt \tag{13}$$

The speed is estimated by a PI controller described as:

$$\hat{\omega}_r = K_p (e_{is\alpha} \hat{\phi}_{r\beta} - e_{is\beta} \hat{\phi}_{r\alpha}) + K_i \int (e_{is\alpha} \hat{\phi}_{r\beta} - e_{is\beta} \hat{\phi}_{r\alpha}) dt \tag{14}$$

with K_p and K_i are positive constants. The feedback gain matrix L is chosen to ensure the fast and robust dynamic performance of the closed loop observer [13, 14].

$$L = \begin{bmatrix} l_1 & -l_2 \\ l_2 & l_1 \\ l_3 & -l_4 \\ l_4 & l_3 \end{bmatrix} \tag{15}$$

with l_1, l_2, l_3 and l_4 are given by:

$$l_1 = (k_1 - 1) \left(\gamma + \frac{1}{T_r} \right) \quad ; \quad l_2 = -(k_1 - 1) \hat{\omega}_r$$

$$l_3 = \frac{(k_1^2 - 1)}{K} \left(\gamma - K \frac{L_m}{T_r} \right) + \frac{(k_1 - 1)}{K} \left(\gamma + \frac{1}{T_r} \right) \quad ; \quad l_4 = -\frac{(k_1 - 1)}{K} \hat{\omega}_r$$

where k_1 is a positive coefficient obtained by pole placement approach [15].

The structure of the observer of states is illustrated by Fig. 6.

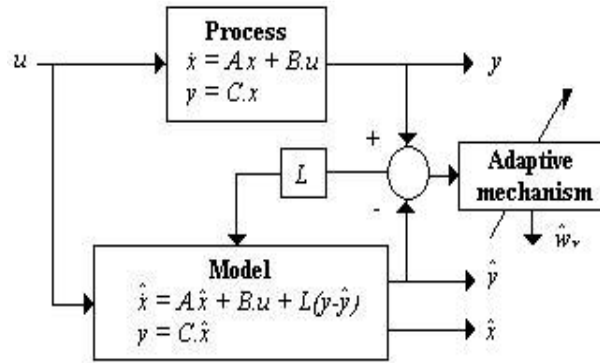


Fig. 6. Block diagram of the adaptive Luenberger observer.

Conventional control techniques require accurate mathematical models and have effect in the presence of uncertainties and unknown external disturbances. In this case, we will replace the PI controller in ALO adaptation mechanism by a fuzzy logic controller.

6. Fuzzy Logic Controlled Adaptive Luenberger Observer

Figure 7 shows the block diagram of fuzzy logic controller system where the variables K_p, K_i and B are used to tune the controller.

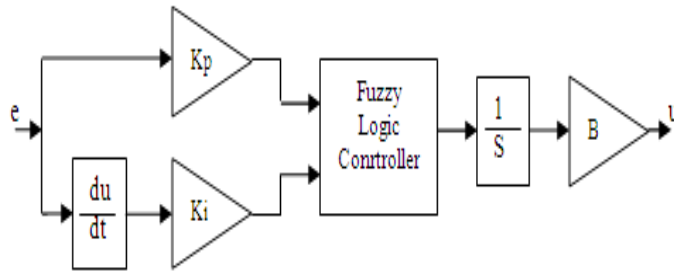


Fig. 7. Block diagram of a fuzzy logic controller.

There are two inputs, the error e and the change of error ce . The FLC consists of four major blocks, Fuzzification, knowledge base, inference engine and defuzzification [16].

6.1. Fuzzification

The input variables e and ce are transformed into fuzzy variables referred to as linguistic labels. The membership functions associated to each label have been chosen with triangular shapes. The following fuzzy sets are used, NL (Negative Large), NM (Negative Medium), NS (Negative Small), ZE (Zero), PS (Positive Small), PM (positive Medium), and PL (Positive Large). The universe of discourse is set between -1 and 1 . The membership functions of these variables are shown in Fig. 8.

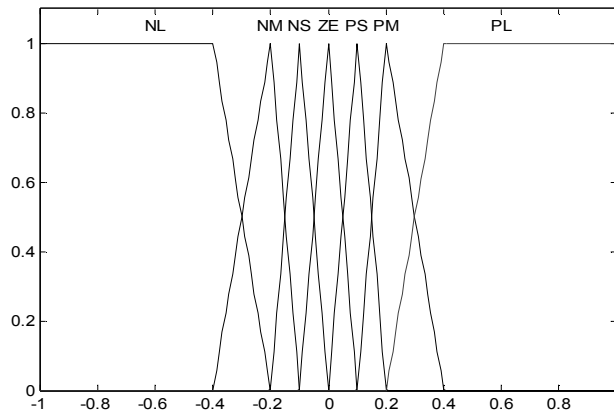


Fig. 8. Membership functions.

6.2. Knowledge base and inference engine

The knowledge base consists of the data base and the rule base. The data base provides the information which is used to define the linguistic control rules and the fuzzy data in the fuzzy logic controller. The rule base specifies the control

goal actions by means of a set of linguistic control rules [17]. The inference engine evaluates the set of IF-THEN and executes 7*7 rules as shown in Table 2. The linguistic rules take the form as in the following example:

IF e is NL AND ce is NL THEN u is NL

Table 2. Fuzzy rule base.

ce/e	NL	NM	NS	ZE	PS	PM	PL
NL	NL	NL	NL	NL	NM	NS	ZE
NM	NL	NL	NL	NM	NS	ZE	PS
NS	NL	NL	NM	NS	ZE	PS	PM
ZE	NL	NM	NS	ZE	PS	PM	PL
PS	NM	NS	ZE	PS	PM	PL	PL
PM	NS	ZE	PS	PM	PL	PL	PL
PL	ZE	PS	PM	PL	PL	PL	PL

6.3. Defuzzification

In this stage, the fuzzy variables are converted into crisp variables. There are many defuzzification techniques to produce the fuzzy set value for the output fuzzy variable. In this paper, the centre of gravity defuzzification method is adopted here and the inference strategy used in this system is the Mamdani algorithm.

7. Simulation Results

A series of simulation tests were carried out on direct torque control of induction motor based on the adaptive Luenberger observer using fuzzy logic controller in adaptation mechanism. Simulations have been realized under the Matlab/Simulink. The parameters of induction motor used are indicated in Table 3.

Table 3. Induction motor parameters.

Rated power	3 kW
Voltage	380V Y
Frequency	50 Hz
Pair pole	2
Rated speed	1440 rpm
Stator resistance	2.2 Ω
Rotor resistance	2.68 Ω
Stator inductance	0.229 H
Rotor inductance	0.229 H
Mutual inductance	0.217 H
Moment of inertia	0.047 kg.m ²
Viscous friction	0.004 N.m.s/rad

7.1. Operating at load torque

Figures 9 to 14 represents the simulation results obtained from a no load operating. We impose a speed of reference of 100 rad/s and we applied a load torque with 10 N.m between $t = 0.5$ s and $t = 1.5$ s.

7.2. Operating with inversion of the speed

We applied a speed reference varying between 100 rad/s to -100 rad/s. The simulation results are illustrated by Figs. 15 to 18.

7.3. Operating at high speed

Figures 19 to 22 illustrate simulation results when a rotor speed of 157 rad/s is imposed.

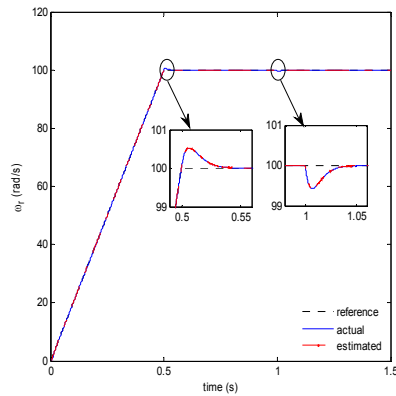


Fig. 9. Responses of speed.

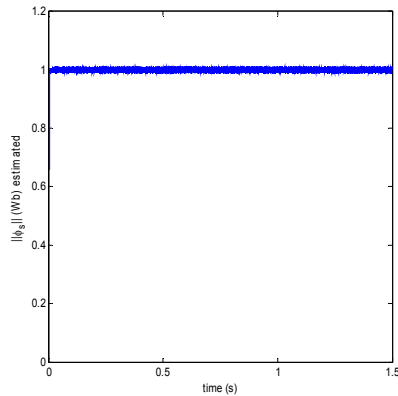


Fig. 10. Estimated stator flux.

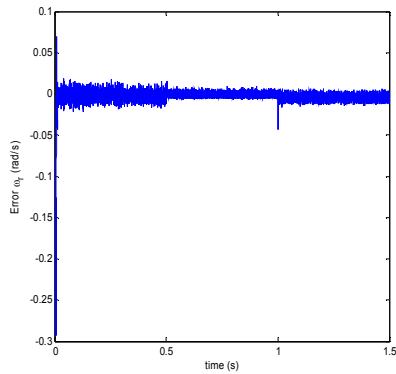


Fig. 11. Speed error.

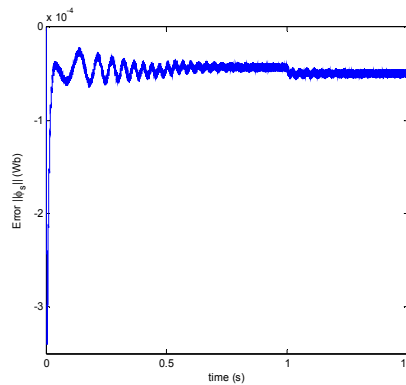


Fig. 12. Flux error.

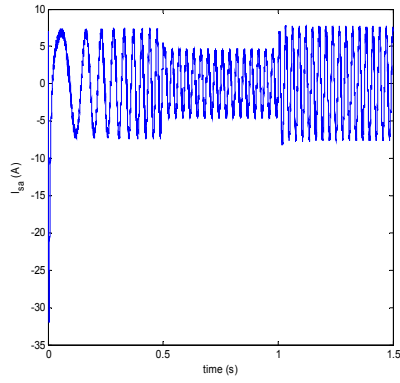


Fig. 13. Stator phase current.

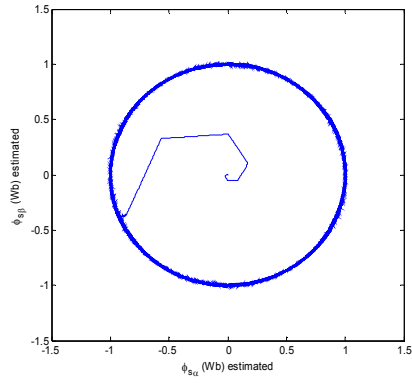


Fig. 14. Trajectory of estimated stator flux components.

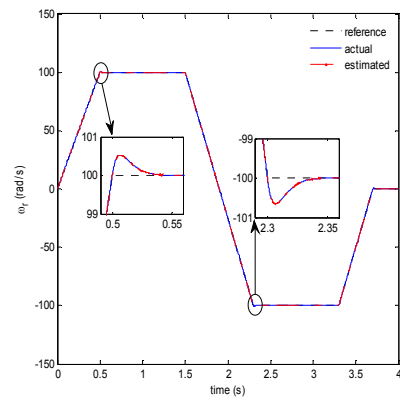


Fig. 15. Responses of speed.

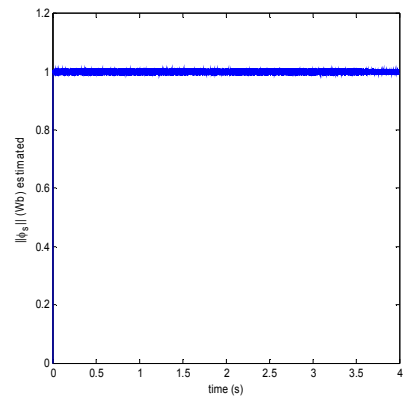


Fig. 16. Estimated stator flux.

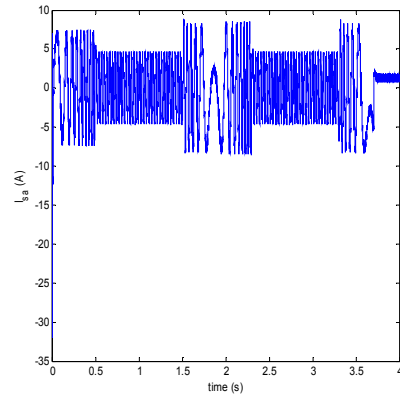


Fig. 17. Stator phase current.

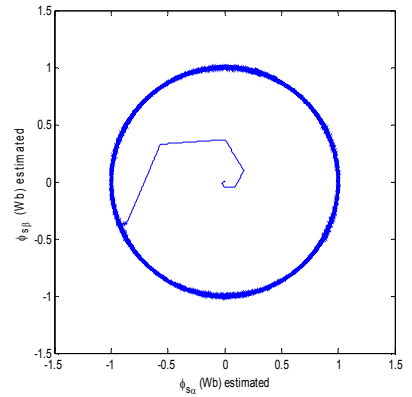


Fig. 18. Trajectory of estimated stator flux components.

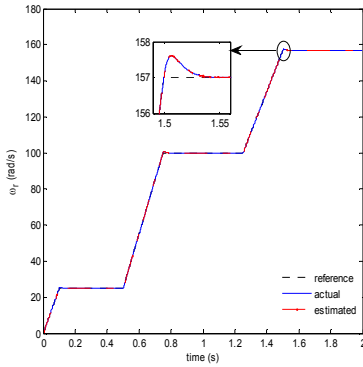


Fig. 19. Responses of speed.

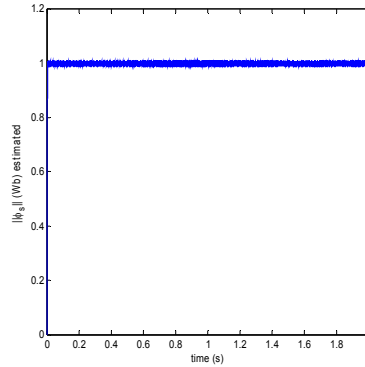


Fig. 20. Estimated stator flux.

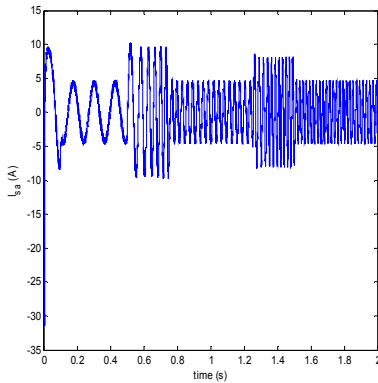


Fig. 21. Stator phase current.

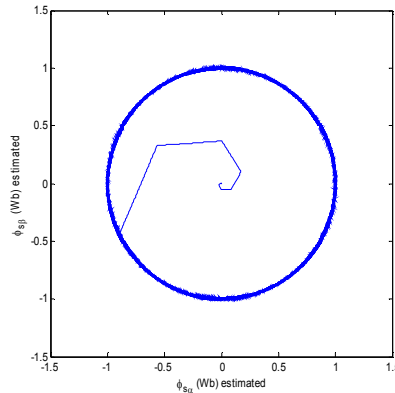


Fig. 22. Trajectory of estimated stator flux components.

7.4. Operating at low speed

Figures 23 and 24 illustrate simulation results with a speed carried out for low speed ± 10 rad/s. With the obtained results above, the estimated speed follows the reference speed closely. The stator phase current in the induction motor remains sinusoidal and takes appropriate value. The stator flux vector describes a circular trajectory.

In high and low speed functioning, the estimated speed follows perfectly the speed reference. We can notice good dynamic behavior and steady state responses of flux and speed. The adaptation mechanism of Adaptive Luenberger observer with fuzzy logic controller gives better responses in different working of speed especially in high and low speed. Table 4 shows some general characteristics of the DTC control.

Table 4. Summarizing the performances.

Performances	DTC
Ripples flux	Ripples in transient and steady state response
Flux	Fast dynamic response No flux drop
Load rejection	Very quickly

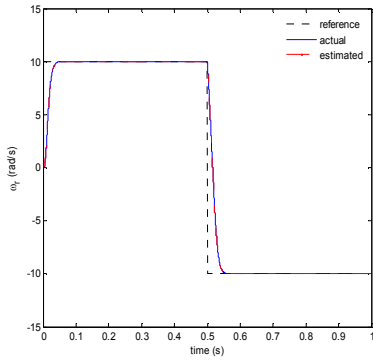


Fig. 23. Responses of speed.

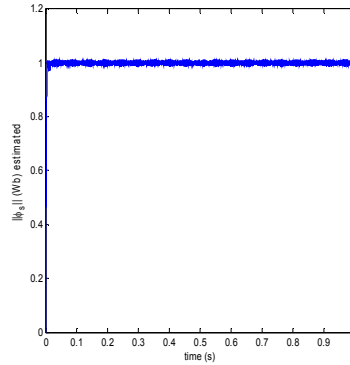


Fig. 24. Estimated stator flux.

8. Conclusion

In this paper we have studied the remarkable performances of an induction motor drive using the sensorless direct torque control with adaptive Luenberger observer based on fuzzy logic for adaptation mechanism. The diagram of the control used allows reducing the ripples of flux and torque and especially improving the performances of the DTC order in high and low speed. The DTC method has a faster dynamic response due to the absence of the current controller and don't need any speed encoder.

References

1. Abbou, A.; and Mahmoudi, H. (2009). Speed control for induction motor using DTFC strategy and intelligent techniques. *Journal of Electrical Systems*, 5(3), 64-81.
2. Blaschke, F. (1971). The principle of field orientation as applied to the new transvector closed loop control system for rotating-field machines. *Siemens Rev*, 34, 217-220.
3. Bennassar, A.; Abbou, A.; Akherraz, M.; and Barara, M. (2013). Speed sensorless indirect field oriented control of induction motor using an extended Kalman filter. *Journal of Electrical Engineering*, 13(1), 238-243.
4. Takahashi, H.; and Noguchi, T. (1987). A new quick response and high-efficiency control strategy of induction motor. *IEEE Transactions on Industry Applications*, IA-22(5), 820-827.
5. Abbou, A.; Mahmoudi, H.; and Elbacha, A. (2004). The effect of stator resistance variation on DTFC of induction motor and its compensation. *14th IEEE International Conference on Electronics, Circuits and Systems*, 894-898.
6. Idris, N.R.N.; and Yatim, A.M. (2004). Direct torque control of induction machines with constant switching frequency and reduced torque ripple. *IEEE Transactions on Industrial Electronics*, 51(4), 758-767.

7. Belhadj, J.; Slama-Belkhodja, I.; Pietrzak-David, M.; and De Fornel, B. (2003). Direct Torque control of induction machine with a short-time computing observer. *Electromotion*, 10, 449-454.
8. Buja, G.S.; and Kazmierkowski, M.P. (2005). Direct torque control of PWM inverter-fed Ac motors-Asurvey. *IEEE transactions on Industrial Electronics*, 51(4), 744-757.
9. Cao, Y.; Lin, Z.; and Ward, D.G. (2002). An anti-windup approach to enlarging domain of attraction or linear systems to actuator saturation. *IEEE Transactions on Automatic Control*, 47, 140-145.
10. Zaccarian, L.; and Teel, A. (2004). Nonlinear scheduled anti-windup design for linear systems. *IEEE Transactions on Automatic Control*, 47, 2055-2061.
11. Juraj Gacho; and Milan Zalman. (2010). IM based speed servodrive with Luenberger observer. *Journal of Electrical Engineering*, 6(3), 149-156.
12. Maes, J.; and Melkebeek, J. (2010). Speed sensorless direct torque control of induction motor using an adaptive flux observer. *Proc. of IEEE Transactions on Industry*, 36, 778-785.
13. Belkacem, S.; Nacéri, F.; Betta, A.; and Laggoune, L. (2005). Speed sensorless of induction motor based on an improved adaptive flux observer. *IEEE Transactions on Industry Applications*, 1192-1197.
14. Akin, B. (2003). State estimation techniques for speed sensorless field orient control of induction motors. M.Sc. Thesis. EE Department, METU.
15. Sio-Iong Ao Len Gelman. (2009). Advances in electrical engineering and computational science lecture. *Notes in Electrical Engineering*, 39, Editors.
16. Bennassar, A.; Abbou, A.; Akherraz, M.; and Barara, M. (2013). Fuzzy logic speed control for sensorless indirect field oriented of induction motor using an extended Kalman filter. *International Review of Automatic Control*, 6(3), 332-339.
17. Peter, V. (1998). Sensorless vector and direct torque control. *Oxford New York Tokyo, Oxford University Press*.
18. Bennassar, A.; Abbou, A.; Akherraz, M.; and Barara, M. (2014). Applied approach intelligent technique for speed control of induction machine. *The 4th International Conference on Multimedia and Computing systems*, 1008-1014.
19. Belhadj, J.; Salma-Belkhodja, I.; Pietrzak-David, M.; and De Fornel, B. (2003). Direct torque control of induction machine with a short-time computing observer. *Electromotion*, 6, 449-454.